Nanoparticle Formation within Dendrimer-Containing Polymer Networks: Route to New Organic−Inorganic Hybrid Materials

Franziska Gröhn, Ginam Kim, Barry J. Bauer, and Eric J. Amis*

Polymers Division, National Institute of Standards and Technology, Gaithersburg, Maryland 20899

Received August 28, 2000; Revised Manuscript Received December 29, 2000

ABSTRACT: Higher generation poly(amidoamine) (PAMAM) dendrimers have the unique ability to act as templates for the formation of inorganic nanoclusters. Here, we use dendrimers dispersed in a polymer matrix to create a new type of polymer−inorganic composite material. Hydrophilic polymer networks (poly(2-hydroxyethyl methacrylate)) that contain poly(amidoamine) dendrimers were swollen in aqueous solution, and metal ions were attached to the dendrimers. Chemical reduction on these precursor ions results in nanoparticles that are located inside the dendrimers, which are dispersed in the polymer matrix. Small-angle X-ray scattering (SAXS) and transmission electron microscopy (TEM) were used to characterize gold, platinum, and copper nanoclusters within the polymer networks. These new organic−inorganic hybrid materials may be important for a combination of optical or catalytic properties of the colloids with the mechanical properties provided by the polymer network.

I. Introduction

Because of quantum size effects, inorganic nanoparticles have unique and size-dependent optical, electrical, and magnetic properties that can lead to a wide variety of practical applications. In solution, discrete nanoparticles of differing chemical compositions with narrow size distribution can be synthesized in a classical way using low molecular mass molecules to stabilize the growing colloidal structure or in a more controlled way via the synthesis in confined reaction media such as microemulsions or block copolymer micelles. However, certain applications may require a solid polymeric matrix in order to combine the special colloidal effects with the mechanical properties of the surrounding polymer. Making the synthesis of such solid composite materials amenable to practical use has remained elusive. In general, two approaches can be considered: The initial synthesis of spherical nanoparticles in solution can be followed by further processing such as solvent evaporation or molecular cross-linking. On the other hand, solid polymeric materials such as polymer gels can be directly used as a matrix for the formation of inorganic nanoparticles. This method has recently been used for the preparation of a magnetic mineral/polymer composite consisting of an elastic polystyrene−polyacrylate copolymer gel that contains magnetic iron oxide colloids.[1] These "elastic magnets" demonstrate the ability to combine the desired properties of inorganic and polymeric components in an inorganic−organic hybrid material.

The formation of inorganic colloids within such polymer matrices yields composite materials with exciting and promising properties, but it does not allow for an independent control of the number density or distribution and size of the inorganic particles. To understand the fundamental behavior of hybrid nanostructures such as formation mechanisms or properties, it is desirable to be able to create nanoparticles with a defined concentration and size inside a polymeric matrix. In addition, it is necessary to be able to fully characterize the nanometer scale structure of such hybrid materials. The disadvantages of the systems mentioned above could be overcome by the combination of a well-defined template and a polymer matrix prior to the synthesis of nanoparticles inside this "template−matrix".

Recently, poly(amidoamine) (PAMAM) dendrimers, polymer molecules in the size range of 1−15 nm, have been successfully used as stabilizers and templates for inorganic nanoclusters in aqueous or methanol solution.[2−13] In this approach, precursor ions are accumulated within the dendrimer molecule due to electrostatic attraction[3,9,13] or coordination to its amine groups.[2,4,5,7,8] For higher generation dendrimers, chemical reactions on these precursor ions lead to the formation of inorganic colloids that are located inside individual dendrimers.[13]

This system is different than the confined reaction spaces of micellar systems, since it is not based on hydrophobic−hydrophilic interactions for the confinement, but a reaction takes place in a homogeneous, hydrophilic (aqueous) solution. The concept of nanotemplating by charged, solvent-penetrable nano-polymer particles in aqueous solution had first been applied to the synthesis of gold nanonetworks in poly(styrenesulfonic acid) microgels.[14] In contrast to the results with that system, dendrimer nanotemplates allow for the control of the number of ions that form one colloidal particle. No redistribution of gold ions upon reduction was found in solution, an observation we have referred to as a "fixed loading law".[13] Therefore, in solution, the size of the inorganic particle formed inside the dendrimer can be precisely controlled via dendrimer generation and loading ratio.

The aim of this study is to investigate "dendrimer nanotemplating" transferred to solid materials. Recently, it has been shown that PAMAM dendrimers can permeate into a copolymer film resulting in dendrimer/polyanhydride composite thin films[15] and further that PAMAM dendrimers can be uniformly dispersed in a hydrophilic polymer network by the use of an interpenetrating polymer network synthesis.[16] In this method, 2-hydroxyethyl methacrylate (HEMA) containing a mass fraction of 0.1−10% PAMAM dendrimer and 0.5% ethylene glycol dimethacrylate as cross-linker has been polymerized resulting in a poly-HEMA (PHEMA) network with dispersed PAMAM dendrimers. These den-

10.1021/ma001489j
Published on Web 03/02/2001

drimer−polymer networks are potential precursors for the production of inorganic colloids within a polymeric matrix. The approach is based on the swollen polymer network allowing for metal ions to accumulate inside the dendrimer when exposed to aqueous metal salt solution. In analogy to the dendrimer nanotemplates in solution, chemical reactions on these precursor ions should yield inorganic nanoparticles inside the dendrimers, i.e., dispersed in the polymer matrix. We use small-angle X-ray scattering (SAXS) and transmission electron microscopy (TEM) for the characterization of the hybrid materials formed.

II. Experimental Section

Synthesis. PAMAM dendrimers[17,18] were obtained from Dendritech (Michigan Molecular Institute) as a solution in methanol (dendrimer mass fraction of 20−25%).[19] The dendrimer−polymer networks were prepared by dissolving the dendrimers in HEMA containing a mass fraction of 0.5−1% ethylene glycol dimethacrylate with AIBN as an initiator for the methacrylate. They were polymerized at 35 °C for 72 h and at 70 °C for an additional hour.

The dendrimer−polymer networks were swollen in water and cut into small pieces of about 1 mm thickness. The polymer pieces were placed into aqueous solutions of $HAuCl_4$, H_2PtCl_6, or $Cu(NO_3)_2$ (2×10^{-6}−1×10^{-4} M) for 1 week.[20] Afterward, the network was transferred in water or 0.1 M hydrochloric acid, with this solution replaced every day for about 2 weeks, until no further gold salt was washed out, as was judged by eye from the color of the solution. For the investigation of the metal−salt loaded materials, samples were then dried in a vacuum. For the synthesis of metal nanoclusters, the network pieces were transferred into a solution of reducing agent, e.g., sodium borohydride in 0.2 M NaOH solution, and then washed again with water and finally dried in a vacuum.

Small-Angle X-ray Scattering (SAXS). SAXS data were collected at the Advanced Polymer Beamline at Brookhaven National Laboratory, X27C. The radiation spectrum from the source was monochromated using a double multilayer monochromator and collimated with three 2° tapered tantalum pinholes to give an intense X-ray beam at $\lambda = 1.307$ Å.[21] A 2D image plate detector (BAS2000, Fuji) was used. The sample-to-detector distance was varied between 1 and 1.5 m. A vacuum chamber was placed between the sample and detector to reduce air scattering and absorption. The span of scattering vector magnitudes ($q = (4\pi/\lambda)\sin(\theta)$ where 2θ is the scattering angle) was in the range $0.15\ \text{nm}^{-1} < q < 3.2\ \text{nm}^{-1}$ and $0.2\ \text{nm}^{-1} < q < 4.4\ \text{nm}^{-1}$ for the two configurations used. Scattering patterns from silver behenate and Lupolen were used for angular and absolute intensity calibration of the detectors. A parallel plate ionizing detector placed before the sample cell was used to monitor the incident intensities. The experimental intensities were corrected for incident intensity and for background scattering from the camera and empty cell. The correction for pixel-by-pixel detector sensitivity was established from the scattering of an Fe-55 source.

The two-dimensional data were circularly averaged. Uncertainties were calculated from the standard deviation of the pixel statistics in the averaged annulus. The scattering curves presented here were obtained by further averaging curves from three individual measurements. The uncertainties are the standard deviations of the mean intensity and are plotted only when the uncertainty limits are larger than the size of the plotted data points. All scattering intensities were corrected for solvent scattering.

The scattering curves $I(q)$ were Fourier transformed into the pair distance distribution function $P(r)$ using the program ITP (*Indirect Transformation for the Calculation of* $P(r)$) by Glatter.[22−24] This includes smoothing of the primary data by a weighted least-squares procedure (estimation of the optimum stabilization parameter based on a stability plot) and transformation into real space by the indirect transformation method with minimized termination effects.

Transmission Electron Microscopy (TEM). Samples were ultramicrotomed at −30 °C with a range of thickness from 60 to 80 nm and transferred to carbon-coated copper grids (200 mesh). Staining of these thin sections was performed by inverting the grid on a drop of aqueous phosphotungstic acid solution that had been neutralized with NaOH (mass fraction of 2% phosphotungstic acid). The grid was then blotted on filter paper and air-dried. TEM images were obtained with a Phillips 400 T at 120 kV using low-dose conditions at a magnification of 17 000× and 36 000×.

III. Results and Discussion

Poly(2-hydroxyethyl methacrylate) networks containing dispersed dendrimers are clear and transparent materials, in a dried as well as in a water-swollen state. When exposed to metal salt solutions, the swollen polymer networks turn into the color of the solution, e.g., yellow and brown using $HAuCl_4$ and H_2PtCl_6, respectively, indicating the diffusion of the metal salt solution into the network. In the case of copper salt, the network turns dark blue, which in addition indicates the coordination of the copper ions to the dendrimer amine groups.

The three metal salts used have differing attachment mechanisms of the metal ions to the dendrimer. The $AuCl_4^-$ ion does not show specific interaction with amine groups and is attracted by the dendrimer via electrostatic interaction. This approach has allowed the formation of gold nanoclusters in dendrimers in aqueous solution as shown previously.[13] Conversely, the Cu^{2+} ions are attracted by coordination chemistry, and no attraction via opposite charge is present. For solutions, the complexation of copper ions to PAMAM dendrimers has been previously studied by EPR and UV−vis spectroscopy, showing that metal ions can be coordinated to outer primary as well as inner tertiary dendrimer amine groups.[2,3,25−27] Further, $PtCl_6^{2-}$ ions should have both electrostatic attraction and coordination to the dendrimer amine groups.

The use of platinum salt allows investigation of the salt loaded dendrimer−polymer networks by SAXS. The platinum ions provide the contrast in the X-ray experiment. Figure 1 shows results for dendrimer−polymer networks containing a mass fraction of 1% dendrimers of different generation, generation 7−10 (G7−G10), after loading with H_2PtCl_6. The scattering curves exhibit the features typical of the form factors of these higher generation dendrimers in solution, i.e., sphere form factors.[28] This result demonstrates that the $PtCl_6^{2-}$ ions are indeed accumulated inside the dendrimer. In addition, it can be seen from the scattering curves that the dendrimers are well-dispersed inside the polymer matrix, and no aggregates are detected. This is in agreement with recent SAXS and TEM characterization of these unmodified dendrimer−polymer networks under staining with phosphotungstic acid.[16] The same result is found for loading the networks with copper ions.

For a quantitative analysis, we have also Fourier transformed the scattering curves into pair distance distribution functions, $P(r)$. This is possible in this case of a solid material under the condition of noninteracting particles (dendrimers loaded with metal salt) that are randomly oriented in a homogeneous matrix; i.e., the scattering patterns are analogous to particle solutions. Figure 1b displays the pair distance distribution functions corresponding to the scattering curves in Figure 1a, which represent homogeneous spheres with diameters of 8.5, 11, 13, and 15.5 nm for the G7, G8, G9,

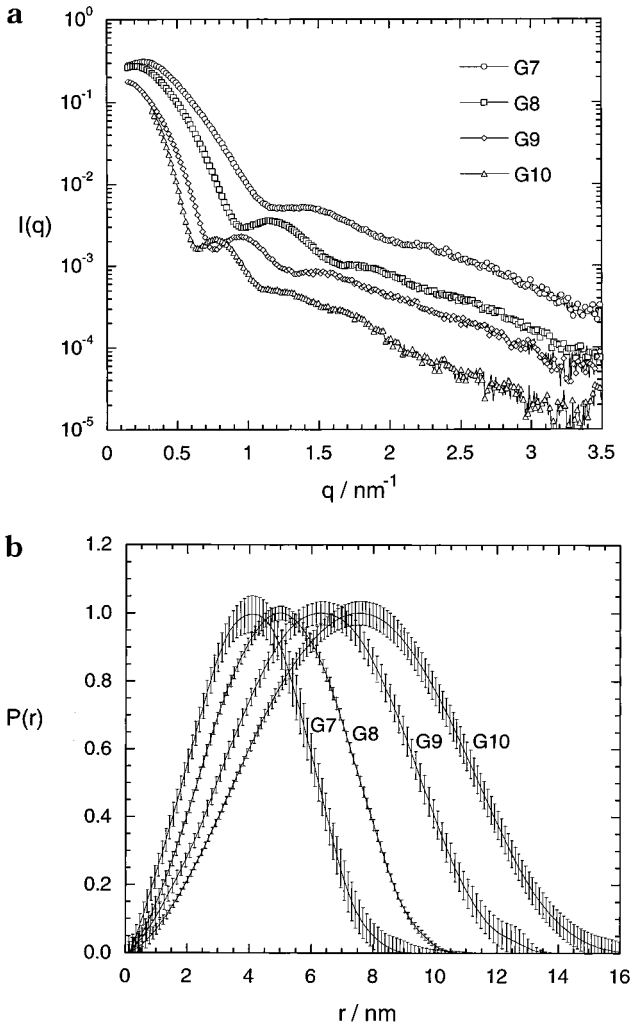

Figure 1. (a) Small-angle X-ray scattering curves $I(q)$ of dendrimer−polymer networks loaded with H_2PtCl_6 for dendrimers of different generation, G7−G10 (mass fraction of 1% dendrimer). Scattering curves were shifted in order to allow for a better comparison and thus do not represent absolute intensities in this plot. The relative standard deviation in the SAXS intensity values for $q < 1.5$ nm^{-1} is less than 1%. At higher wavevectors, the relative standard deviation increases with q to a maximum value of 15%. (b) Normalized pair distance distribution functions $P(r)$ obtained by indirect Fourier transformation of the scattering data $I(q)$ (program ITP). Homogeneous sphere structures with different diameters become evident, indicating that metal ions are accumulated inside the dendrimers. Error bars are the standard deviation in the estimation of $P(r)$, which results from the fit to the $I(q)$ data in (a).

and G10 dendrimer, respectively. The sizes of the platinum salt loaded dendrimers within the polymeric matrix correspond to the sizes of these dendrimers in aqueous solution that were measured previously.[28] In addition, in a recent study on these dendrimer-containing polymer networks we found the same sizes for the dispersed dendrimers stained with phosphotungstic acid by TEM and by SAXS through the location of the minimum in the scattering curve before the first higher order feature.[16] Thus, for the samples investigated here, the association of $PtCl_6^{2-}$ ions with the dispersed dendrimers is confirmed.

Figure 2 shows SAXS data for a metal salt loaded network containing a mass fraction of 10% G8 dendrimer. In this case, the interparticle correlation becomes evident within the q range covered by the

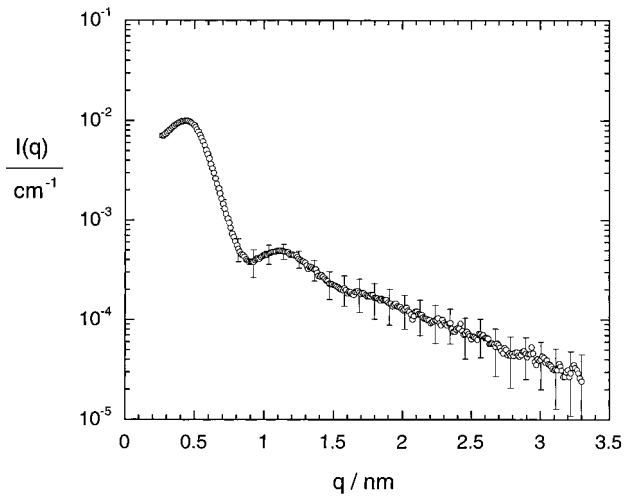

Figure 2. Small-angle X-ray scattering curve $I(q)$ for a dendrimer−polymer network that contains a mass fraction of 10% G8 dendrimer, loaded with copper salt. The peak at low q indicates the interparticle correlations. Error bars are the measured standard deviation in $I(q)$.

measurement. The peak at low q is caused by a peak in the interparticle structure factor $S(q)$, and the position allows for the determination of an experimental interparticle distance d_{exp}. In a simple approximation this is given by $d_{exp} = (3/2)^{1/2}2\pi/q_{max}$. The data in Figure 2 yield an experimental inter-dendrimer distance of 19 ± 1 nm. This value for d_{exp} can further be compared to the distance expected for uniform particle distribution d_{uni}. For a mass fraction (which can be regarded as roughly equal to the volume fraction) of 10% G8 dendrimers, the expected distance for uniform distribution $d_{uni} = (1/\phi v_{den})^{1/3}$ (ϕ volume fraction, v_{den} dendrimer volume) is $d_{uni} = 19.1$ nm. This result confirms the assumption of a homogeneous distribution of dendrimers within the polymer network. Further, the scattering curves for the samples with 1% mass fraction of G7 and G8 dendrimer in Figure 1a also show slight peaks at low q, giving approximate inter-dendrimer spacings of $d_{exp} = 32 \pm 1$ nm and $d_{exp} = 39 \pm 2$ nm for G7 and G8, respectively. These again correspond to the expected distances for uniform particle distribution of $d_{uni} = 32.2$ nm for G7 and $d_{uni} = 41$ nm for G8. Thus, the spacing between the dendrimers is apparently controlled as expected by the dendrimer concentration within a range from 1 to 10%. For G9 and G10 (mass fraction of 1% dendrimer), d_{uni} does not lie within the q range of the SAXS measurement and could not be checked.

Reduction of metal salt inside the polymer−dendrimer network results in metal clusters of nanometer size, as can be seen by the dark red or brown color of the polymer network for the gold and the platinum samples, respectively. It should be noted that gold in the form of colloidal particles is formed only if the polymer network is intensively washed prior to reduction. This is a consequence of excess gold salt in the network that must be removed. In addition, it was necessary to adjust the reduction speed by varying the pH of the reducing solution. This has been previously discussed for the solution experiments.[13,14] For these solid samples, we have chosen sodium borohydride in 0.2 M NaOH solution for reduction. Figure 3 shows TEM images of gold colloids obtained upon reduction of a polymer−dendrimer network that contains a mass fraction of 1% G8 dendrimer. Figure 3a is a sample that was obtained after washing the gold loaded sample with

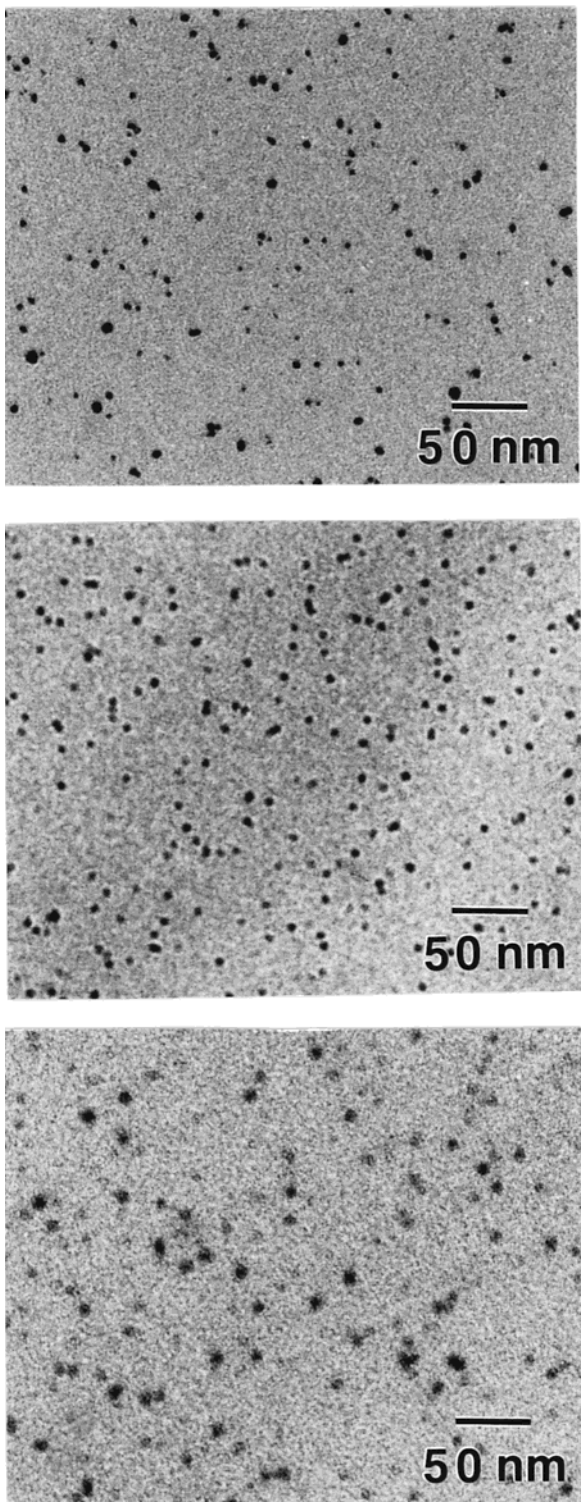

Figure 3. TEM of G8-dendrimer−polymer networks containing gold colloids (mass fraction of 1% dendrimer): (a) reduction of gold after washing the network with water; (b) reduction of gold after washing the network with 0.1 M HCl; (c) sample as in (b) under staining of the dendrimer with osmium tetroxide.

water and Figure 3b after washing with acid. The colloids formed in the case of the acid washing are much more monodisperse, confirming the electrostatic attraction mechanism of ions to the dendrimer. To keep the ions attached to the dendrimer, one has to keep the dendrimer at its maximum charge when washing; otherwise, gold ions are washed out from the matrix and also out of the dendrimer.

The metal colloids that are formed are well-dispersed in the polymer matrix. It should be noted that TEM is a 2D projection of colloids in different layers of the 60−80 nm microtomed section. Although the 2D TEM image may be misleading in terms of interparticle distances, it allows a direct visualization of the particles and measurement of their size and indicates the size distribution. Figure 3c shows the same gold colloid sample after the dendrimer is stained with osmium tetroxide. The dendrimer thus becomes visible in TEM. Under these staining conditions one cannot distinguish between dendrimer and metal particles. The TEM image (Figure 3c) shows only the stained G8 dendrimers of 11 nm size; no additional gold colloids (of the size seen in the unstained sample in Figure 3b) are visible. In addition, the number of dendrimers seen approximately corresponds to the number of gold colloids seen in Figure 3b. We conclude that the gold colloids are formed inside the dendrimers and not in the polymer matrix.

The formation of gold nanoclusters inside the dendrimers is in analogy to our previous results in solution. One might note that while a complexation of metal ions might take place preferably to primary amine groups, an association due to electrostatic attraction, i.e., via counterion condensation, to a penetrable spherical macroion is expected to neutralize inner charges first ("Faraday cage"). However, this is a speculation at this point, and the reason for the inclusion of nanoparticles inside the dendrimers is perhaps even more likely due to a more effective surface stabilization of the formed colloid, rather than the exact precursor structure.

The size range of the gold colloids is 4.0−4.3 nm. It is interesting to compare the size of the gold colloids to previous dendrimer nanoclusters in aqueous solution.[13] In solution, we found that the maximum possible loading with gold ions without causing aggregation of dendrimers corresponded to a molar ratio of dendrimer end groups to gold ions of 1:1. It is important to emphasize that we refer to the number of end groups as a reference value only and do not imply any specific binding to the end groups. The dendrimer contains an equivalent number of inner, tertiary amine groups. The gold ions added per dendrimer molecule could then be reduced to form one colloidal particle ("fixed-loading law"). The resulting colloid sizes were approximately 3.2 nm corresponding to 1000 atoms for G8 and 4.0 nm corresponding to 2000 atoms for G9. Thus, the colloids formed in the dendrimers within a polymer matrix are remarkably larger for the same G8 dendrimer. It is also the case here that the gold salt concentration in the surrounding solution was an order of magnitude larger than necessary for stoichiometric loading. Colloids of 4 nm size consist of about 2000 gold atoms. We note that this corresponds to the total number of chargeable amine groups of one dendrimer molecule (primary and tertiary ones) and could be consistent with the electrostatic attraction mechanism. This would be in contrast to nanotemplating in solution and yield a maximum loading with gold ions which is twice as high. While dendrimers in solution can aggregate upon loading with metal salt, the polymer matrix evidently immobilizes the dendrimers, preventing aggregation. Thus, the association of metal ions with individual dendrimers is possible to this higher loading level which yields larger metal nanoparticles than could be obtained in solution.

Platinum nanoparticles formed inside a G8 dendrimer in the polymer network have a size of 3 nm. This

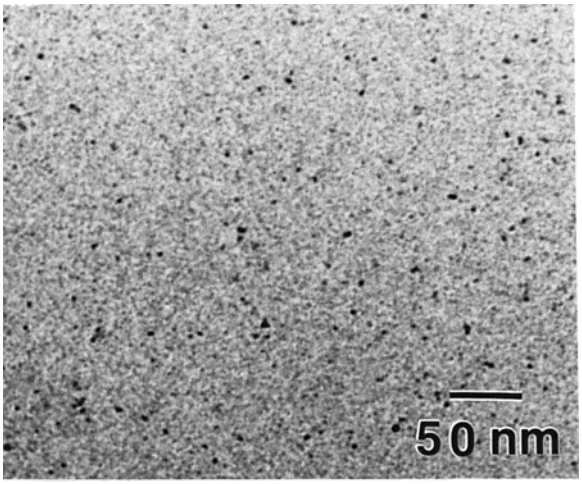

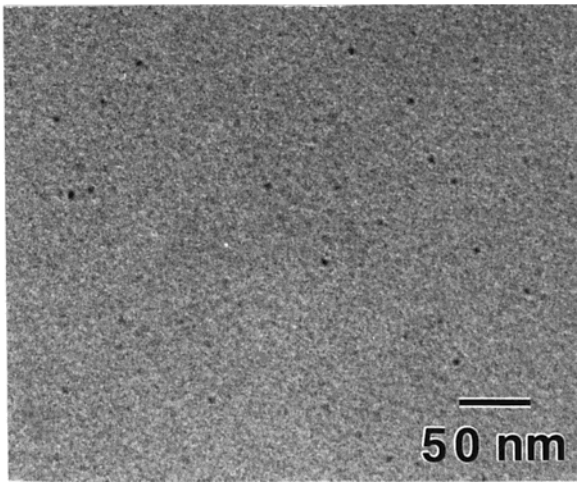

Figure 4. (a) TEM of G8-dendrimer−polymer networks containing platinum colloids (mass fraction of 1% dendrimer). (b) TEM of G8-dendrimer−polymer networks containing copper colloids (mass fraction of 1% dendrimer).

corresponds to about 1000 platinum atoms per nanocluster. The observation of only half as many ions being reduced to form one particle for the platinum as compared to the gold is consistent with the electrostatic attraction mechanism postulated above. Since the $PtCl_6^{2-}$ is doubly charged, as compared to the single charged $AuCl_4^-$, this again corresponds to a one-to-one ratio of amine groups to ion charges. However, as stated before, for platinum ions complexation by amine groups is well-known. We note that this study is focused on the characterization of nanostructures, rather than the exact classification of chemical bonds.

We have also produced copper colloids inside the dendrimer network by the same procedure. A TEM is shown in Figure 4b showing nanoparticles of 3.3 nm diameter, dispersed in the polymer matrix. The lower electron contrast of Cu could mean that fewer colloids are visible by TEM and might be one possible reason for the particle density being apparently lower than in the case of the gold sample. More importantly, we have noted that the copper colloids produced inside the swollen polymer gel are stable for at least several days when exposed to water that may contain dissolved oxygen. This is a remarkable result, since colloidal copper particles usually are not stable in an aqueous environment in the presence of oxygen.[29,30] This suggests an effective colloid surface stabilization is provided by the dendrimer. Previous studies on the preparation

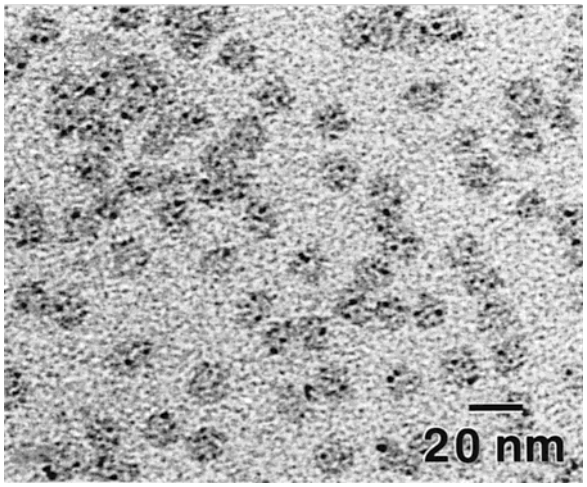

Figure 5. TEM of G9-dendrimer−polymer networks containing platinum colloids (mass fraction of 1% dendrimer). The dendrimers have been stained with phosphotungstic acid and appear gray, and the platinum colloids appear black.

of dendrimer-stabilized metal nanoclusters have also demonstrated a stability of copper colloids in oxygen-free aqueous solution;[2,4] however, in air-saturated solution the clusters were converted into dendrimer coordinated copper ions overnight. The copper−dendrimer−polymer composites may thus have potential in special applications that otherwise cannot be easily realized, for example the use of a colloidal copper catalyst in aqueous solution.

We approximate the size of the copper nanoclusters as 3.3 nm, which, using our previous estimations, corresponds to a ratio of between one and two amine groups per copper ion. Because of the lower contrast of the copper (as compared to gold and platinum) inside the polymeric matrix, we are not confident of the size of the copper nanocluster, and we report it here for comparison only. The coordination of dendrimer amine groups to metal ions under different conditions in solution has been recently studied by Ford et al. using spectrophotometry,[25] and we have not attempted to repeat these investigations for this system.

For the case of platinum clusters we have used dendrimers of different generations to investigate the attachment of the ions and the reduction of the ions into metal nanoclusters. For this purpose, we produced platinum nanoclusters in polymer−dendrimer networks containing G7, G8, G9, and G10 PAMAM dendrimers, each with a dendrimer mass fraction of 1%. Results for the salt loaded precursor samples are shown in Figure 1. For the G7 sample, after reduction, we find platinum clusters of approximately 2.4 nm diameter, corresponding to about 500 platinum ions. This is consistent with the results for the G8 sample with two positively charged amine groups attracting one $PtCl_6^{2-}$ ion and the control of particle size determined by the precursor ions on the dendrimers.

In contrast, for G9 and G10, multiple smaller platinum clusters inside one dendrimer are formed. Figure 5 shows an example of platinum colloids inside G9 dendrimers, where the dendrimers have been stained with phosphotungstic acid in order to visualize both the platinum (black) and the dendrimer (gray) within the PHEMA matrix. This change in the morphology of the nanoclusters with dendrimer generation is also observed by SAXS. Figure 6a shows pair distance distribution

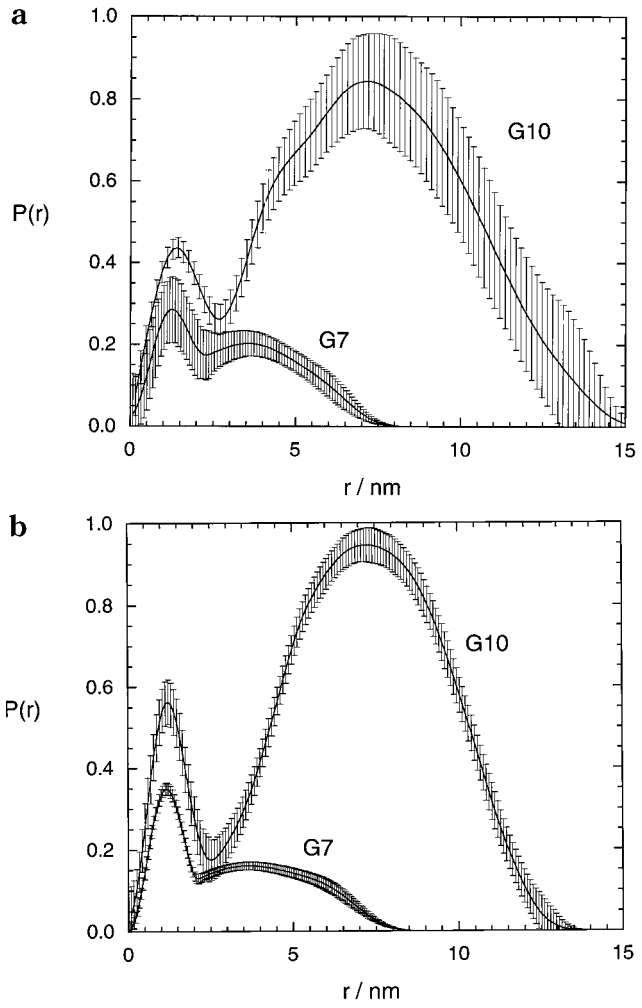

Figure 6. SAXS pair distance distribution functions $P(r)$ for G7 and G10 dendrimers: (a) for platinum nanoclusters in polymer−dendrimer networks; (b) for gold nanoclusters in dendrimers in solution.[13] For both systems, the shape of the $P(r)$ function, specifically the relative peak height, changes with dendrimer generation. This is caused by the formation of one colloid per dendrimer for G7 but multiple colloids for G10. Error bars are the standard deviation in the estimation of $P(r)$, which results from the fit to the measured $I(q)$ data.

functions for platinum nanoclusters in dendrimer−polymer networks for both G7 and G10. The $P(r)$ reveals a layered-sphere structure in both cases. However, for the G7 dendrimer a deviation from a strict spherical symmetry becomes evident from the relative peak heights in the $P(r)$ functions.[13] We have previously demonstrated that such a deviation can be caused by the location of a single metal colloid inside a dendrimer with an offset from the center.[13] The difference in relative height of the first and second peak in $P(r)$ in G7 and G10 is due to the formation of single (off-center-placed) and multiple particles, respectively.

To understand this generation-dependent behavior, we can consider different factors influencing nanocrystal growth. In general, the growth of a colloid is determined by the free energy of the crystal formation and surface tension. When the colloid grows inside a polymeric template, the forces of the surrounding polymer become important, and the growth of a nucleated colloid is limited by the finite extension of neighboring polymer chains. The mass of the dendrimer molecule doubles with each generation, while the size increases only linearly; i.e., the internal dendrimer segment density increases, and the chain flexibility decreases. Conversely, under the fixed loading assumption the volume of a single gold nanocluster would double with each generation. For the highest generation dendrimers, it may be that the space available and the chain flexibility are not sufficiently high to allow growth of one single colloidal particle. On the other hand, the increased surface to be stabilized for multiple smaller particles is likely to be provided by the segments of the dendrimers. We can thus rationalize that the different volume conditions inside the dendrimer cause the formation of different colloid morphologies. A similar transition of the morphology with dendrimer generation was found for the nanotemplating in solution.[13] Even if the morphology change is a general phenomenon, the transitions could depend on the systems. The G9 gold sample in solution yields a single metal colloid, but the G9 platinum sample in the network yields multiple particles. In both cases the number of ions per G9 dendrimer is approximately 2000, and the size of a single colloid would be approximately 4 nm. This suggests that the polymer matrix, in addition to the dendrimer itself, plays a role in the process of colloid formation. From the mechanism of the network formation it might be that the polymer interpenetrates the dendrimer and could therefore contribute to formation of multiple particles rather than a single colloid. SAXS results for the G7 and G10 solution gold samples are given in Figure 6b, showing the similarities between the systems and thus the generality of these factors in dendrimer nanotemplating.

Large-scale production of these polymer−dendrimer−nanoparticle composites does not seem feasible due to the high cost of dendrimers and due to the time scale associated with a synthesis based on diffusion into a polymer gel. In this context it is important to note that it was not possible to produce the same composite materials by using the nanocluster containing dendrimers that were synthesized a priori by nanotemplating in solution. The PAMAM dendrimer containing gold colloid is not soluble in the HEMA monomer. This modulation of dendrimer solubility by an embedded host is an interesting phenomenon and indicates the accessibility of the nanocluster to solvent molecules. However, the new nanocomposites may be of use in special applications that do not rely on large amounts of material, as for example polymer thin films with modified dielectric constant. Regarding applications as catalysts, it has been recently shown that dendrimer stabilized metal colloids in solution can be applied as selective catalysts for substrates that can diffuse into the dendrimer.[6,8] This concept could also be applied for swellable solid dendrimer−polymer systems. In addition, the metal colloid containing polymer pieces may be easily removed from a reaction solution, washed, and recycled.

IV. Conclusions

Cross-linked poly(2-hydroxyethyl methacrylate) containing dispersed PAMAM dendrimers was used as a template−matrix for the formation of inorganic nanoclusters. When swollen in aqueous solution, metal ions were attached to the dendrimers via electrostatic attraction or coordination to its amine groups. Chemically reducing these metal ions results in gold, platinum, or copper nanoclusters that are located inside the dendrimers, which are dispersed inside the polymer matrix,

representing a new type of nanocomposite material. For G7 and G8, the size of the metal nanoclusters is controlled by the maximum number of metal ions that can be electrostatically attached. For G9 and G10, multiple colloidal particles per dendrimer are formed, as can be understood by the volume conditions inside the dendrimer and the additional influence of the polymer matrix.

The gold nanoparticle containing dendrimer−polymer networks may allow for fundamental studies of colloidal effects such as nonlinear optical properties in a well-defined composite material. In addition, it has been shown that different metal nanoclusters can be produced, which opens the possibility for a wide variety of studies on model nanocomposites as well as applications in areas such as catalysis and dielectrics.

Acknowledgment. We thank Dr. Donald Tomalia of MMI for donation of the dendrimers. SAXS measurements were carried out at the Advanced Polymer Beamline X27C at the National Synchrotron Light Source, Brookhaven National Laboratory. We thank Dr. Yvonne Akpalu for introduction into the SAXS facility and Dr. Feng-Ji Yeh and Dr. Lizhi Liu for their assistance in data acquisition. We thank Dr. Catheryn L. Jackson for help with the TEM and Mr. Da-Wei Liu for the synthesis of initial dendrimer−polymer networks as well as Dr. Brent Viers and Dr. Alamgir Karim for discussions. This material is based upon work supported in part by the U.S. Army Research Office under Contract 35109-CH.

References and Notes

(1) Breulmann, M.; Cölfen, H.; Hentze, H. P.; Antonietti, M.; Walsh, D.; Mann, S.; *Adv. Mater.* **1998**, *10*, 237.
(2) Zhao, M.; Sun, L.; Crooks, R. M. *J. Am. Chem. Soc.* **1998**, *120*, 4877.
(3) Esumi, K.; Suzuki, A.; Aihara, N.; Usui, K.; Torigoe, K. *Langmuir* **1998**, *14*, 3157.
(4) Balogh, L.; Tomalia, D. A. *J. Am. Chem. Soc.* **1998**, *120*, 7355.
(5) Sooklal, K.; Hanus, L. H.; Ploehn, H. J.; Murphy, C. J. *Adv. Mater.* **1998**, *10*, 1083.
(6) Zhao, M. Q.; Crooks, R. M. *Angew. Chem., Int. Ed. Engl.* **1999**, *38*, 364.
(7) Beck Tan, N. C.; Balogh, L.; Trevino, S. F.; Tomalia, D. A.; Lin, J. S. *Polymer* **1999**, *40*, 2537.
(8) Zhao, M.; Crooks, R. M. *Adv. Mater.* **1999**, *11*, 217.
(9) Garcia, M. E.; Baker, L. A.; Crooks, R. M. *Anal. Chem.* **1999**, *71*, 256.
(10) Zhao, M.; Crooks, R. M. *Chem. Mater.* **1999**, *11*, 3379.
(11) Esumi, K.; Suzuki, A.; Yamahira, A.; Torigoe, K. *Langmuir* **2000**, *16*, 2604.
(12) Esumi, K.; Hosoya, T.; Suzuki, A.; Yamahira, A.; Torigoe, K. *Langmuir* **2000**, *16*, 2978.
(13) Gröhn, F.; Bauer, B. J.; Akpalu, Y. A.; Jackson, C. L.; Amis, E. J. *Macromolecules* **2000**, *33*, 6042.
(14) Antonietti, M.; Gröhn, F.; Hartmann, J.; Bronstein, L. *Angew. Chem., Int. Ed. Engl.* **1997**, *36*, 2080.
(15) Zhao, M. Q.; Liu, Y. L.; Crooks, R. M.; Bergbreiter, D. E. *J. Am. Chem. Soc.* **1999**, *121*, 923.
(16) Bauer, B. J.; Prosa, T. J.; Kim, G.; Jackson, C. L.; Liu, D. W.; Amis, E. J. Manuscript in preparation.
(17) Tomalia, D. A.; Baker, H.; Dewald, J.; Hall, M.; Kallos, G.; Martin, S.; Roeck, J.; Ryder, J.; Smith, P. *Macromolecules* **1986**, *19*, 2466.
(18) Tomalia, D. A.; Naylor, A. M.; Goddard, W. A. *Angew. Chem., Int. Ed. Engl.* **1990**, *29*, 138.
(19) Certain commercial materials and equipment are identified in this article in order to specify adequately the experimental procedure. In no case does such identification imply recommendation by the National Institute of Standards and Technology, nor does it imply that the material or equipment identified is necessarily the best available for this purpose.
(20) The accepted SI unit of concentration, mol/L, has been represented by the symbol M in order to conform the conventions of this journal.
(21) Hsiau, B. S.; Chu, B.; Yeh, F. *NSLS Newslett.* **1997**, July1.
(22) Glatter, O. *Acta Phys. Austriaca* **1977**, *47*, 83
(23) Glatter, O. *J. Appl. Crystallogr.* **1977**, *10*, 415.
(24) Glatter, O. *J. Appl. Crystallogr.* **1980**, *13*, 7, 577.
(25) Vassilev, K.; Ford, W. T. *J. Polym. Sci., Part A* **1999**, *37*, 2727.
(26) Ottaviani, M. F.; Bossman, S.; Turro, N. J.; Tomalia, D. A. *J. Am. Chem. Soc.* **1994**, *116*, 661.
(27) Ottaviani, M. F.; Montalti, F.; Turro, N. J.; Tomalia, D. A. *J. Phys. Chem. B* **1997**, *101*, 158.
(28) Prosa, T. J.; Bauer, B. J.; Amis, E. J.; Tomalia, D. A.; Scherrenberg, R. *J. Polym. Sci.* **1997**, *35*, 2913.
(29) Dhas, N. A.; Raj, C. P.; Gedanken, A. *Chem. Mater.* **1998**, *10*, 1446.
(30) Clay, R. T.; Cohen, R. E. *New J. Chem.* **1998**, *22*, 745.

MA001489J